Published in AJSE, Vol: 24, Issue:2
Received on 11th May 2026
Revised on 22nd May 2026
Published on 31th May 2026

AIUB JOURNAL OF SCIENCE AND ENGINEERING
ISSN: 1608 - 3679 (print) 2520 - 4890 (Online)
https://doi.org/10.53799/deaa3j54

Optimizing Humanoid Arm Actuation: Motor Selection, Material Trade-offs, and Transition to Low-Inertia Tension-Amplified Mechanisms

M Tanseer Ali, Abir Ahmed, Mredul Khaliduzzaman, Jagannath Bhowmik, and Md. Abdur Rahman

***Abstract*—The optimization of the actuation systems in the humanoid robotic arm is the focus of this research, which considers different factors including motor performance, selection of materials, and innovative mechanisms. By systematically testing a number of Brushless DC (BLDC) motors with different KV ratings and reduction ratios, it was concluded that the 5048 100KV motor with 30:1 cycloidal drive was optimal, with a high KV rating, high efficiency, low weight and low price. According to the voltage analysis, the 24V system doubled the torque, reduced heat generation and increased responsiveness over the 12V system. Comparisons of material properties between 3D-printed PLA+ and aluminum revealed that PLA+ could be used for lightweight prototype making and aluminum could be used for highly loaded parts due to high strength and high precision. The limitations that are faced by the conventional designs (high inertia, mechanical complexity, energy inefficiency) are overcome by proposing to move forward from the conventional design to a Low Inertia Manipulator with High Stiffness and Strength (LIMS). This is a tension amplified mechanism where the tension is amplified using cable driven mechanisms with high torque to weight ratios, low backlash and high compliance as compared to conventional BLDC based mechanisms. The results provide practical guidance in designing a lightweight and energy-efficient robotic arm and indicate that a hybrid approach for the prototyping to production process is necessary and LIMS should be used in the design of next generation humanoid manipulators.**

***Keywords* — Humanoid robotic arm, Brushless DC motor, Cycloidal drive, LIMS, Cable-driven mechanism, PLA+, Aluminum, Torque optimization, Voltage scaling, Forward kinematics, Inverse kinematics, PID control.**

I. INTRODUCTION

A major breakthrough in the study of humanoids is the development of humanoid robotic arms, which have numerous uses such as industrial automation and assistance in the healthcare field. To realize dexterous human-like motion, these systems demand high torque, low inertia, energy efficiency and accurate control. However, typical brushed DC motor and high ratio gearboxes are physically large, mechanically complex, and inefficient, limiting their application in a dynamic environment. New opportunities for innovation have emerged with the recent advances in brushless DC motors (BLDC), additive manufacturing and tension-based actuation. But there are formidable challenges to be faced in combining these technologies and to them into the integrated and high-performance systems. Current literature has mainly concentrated on improving each individual element separately (e.g., motor, material, mechanism, etc.) without taking the interactions between them into account when designing a humanoid arm. For instance, cycloidal drives are reported to be well suited for torque amplification, but have not paid attention to real performance with variable load (e.g., motor KV ratings). Similarly, comparing 3D printed polymers with metals reveals that there are compromises in strength and weight, and no action steps are taken towards getting from a prototype to a product. The analyses for voltage optimization are also still very general and lack the ability to quantify the effect of the power supply scaling on the joint torque, speed, and thermal management. All these are a reminder that designing an integrated approach that combines energy efficiency, materials use and actuation is needed. This study addresses these gaps by systematically and comprehensively exploring the problem of motor selection, material trade-offs, voltage optimization and a proposed next generation actuation framework. The main and novel contribution of this work is the cable-driven, tension amplified actuation mechanism named LIMS (Low Inertia Manipulator with High Stiffness and Strength) which overcomes the inertia, compliance and energy efficiency drawbacks of traditional BLDC-Cycloidal systems. Individual contributions (motor testing, hybrid materials, voltage analysis) are based on existing engineering practice, whereas the integrated design methodology and the LIMS proposal as an integrated alternative framework are the core contributions. Specifically: (1) Three BLDC motors, 5065 275KV, 5048 154KV, and 5048 100KV, have been empirically evaluated under standardized test conditions and compared with each other, and the 5048 100KV was determined to be optimal for load-bearing humanoid joints; (2) A hybrid material strategy with controlled sample testing and literature sourced benchmarks; (3) Voltage scaling analysis to differentiate between gains in electromechanical efficiency and arithmetic voltage effects; (4) The LIMS framework developed through CAD/CAE simulation to set target performance for physical prototype development.

M Tanseer Ali; Dr Anwarul Abedin Institute for Innovation, AIUB, email: tanseer@aiub.edu
Abir Ahmed, Dr Anwarul Abedin Institute for Innovation, AIUB, email: abir.ahmed@aiub.edu;
Khaliduzzaman Mredul, Dr Anwarul Abedin Institute for Innovation, AIUB, email: khaliduzzaman.mredul@gmail.com
Jagannath Bhowmik, Dr Anwarul Abedin Institute for Innovation, AIUB, email: diptobhowmik15@gmail.com
Md. Abdur Rahman, Dr Anwarul Abedin Institute for Innovation, AIUB, email: arahman@aiub.edu

II. RELATED RESEARCH WORKS AND FINDINGS

A. Motor and Gear Systems

When used with BLDC motors, gear reducers continue to be an important part of robotic arm design. Kim et al. [1] showed

that the combination of a low-KV BLDC motor and a cycloidal drive is quite advantageous in terms of reducing backlash and increasing the torque-to-weight ratio. The load-bearing robotic joints were also explored by Zhang et al. [2] who compared BLDC motor-gearbox combinations for these joints, concluding that the lower KV motors performed better at higher voltage for these joints. Complementary efforts for high torque density actuator design have been reported for groups developing proprioceptive actuators, as well as quasi-direct-drive systems, which also prefer high pole counts and low KV motors for their high torque density [1].

B. Hybrid Actuation and Cable-Driven Systems

To enhance compliance and reduce the inertia, a hybrid system which integrates BLDC motors and tendon-driven systems was proposed by Grebenstein et al. [7]. The idea of cable driven arms with high stiffness is introduced by Nakamura et al. [5] as a key concept in the LIMS. Cable-driven mechanisms were covered in [6] where the advantages of low inertia and natural compliance by using cable were emphasized. Taylor et al. [9] also demonstrated the tension amplification effect can be applied to create torque scaling similar to gear reducers with no backlash.

C. Material Selection in Robotics

Smith et al. [3] had already made a comparison of mechanical properties of 3D-printed PLA+ and aluminum, and concluded that the 3D-printed PLA+ was better with regards to weight reduction of 50-70%, with still not being as strong as the metals and resistance to wear. The hybrid design (polymer for non-critical parts and metal for high-stress parts) was suggested by Gupta et al. [4] and was also used in this work, when moving from PLA+ prototypes to aluminum production prototypes.

D. Voltage and Energy Management

The authors of [11] showed that the torque generated from the same BLDC system was almost doubled when the BLDC system's voltage was increased from 12V to 24V and the current drawn from the BLDC was decreased. Kumar et al. [12] highlighted the importance of voltage control for the energy efficiency and mitigating thermal elevation concerns as was observed in the initial setup of 5065 275KV motor.

E. LIMS Framework

Richer et al. [10] gave design guidelines for low inertia arms and suggested cable driven actuation over the traditional gearboxes. Their work confirms the motivation behind the LIMS framework proposed in this paper. Taylor et al. [9] pointed out that LIMS-type mechanisms usually involve customized components, complicating the manufacturing process. The authors would like to note that the list of related work presented here is limited to an interesting subset of the existing literature; other important contributions are the series elastic actuators (SEAs) and variable stiffness actuators (VSAs) developed at DLR and other institutions [8], the proprioceptive actuators developed at MIT, and the work on compliant cable-driven humanoid arms at ETH Zurich. In future journal versions of this work these bodies of work will be engaged much more, and are relevant for the benchmarks provided for the LIMS proposal.

III. III. ROBOTIC HAND 3D DESIGN

The hand was designed in CAD, viewed from a number of different angles, showing articulation and construction. The design includes cylindrical and spherical components that are joined together with carefully designed joints, ensuring the precise fit and functionality of the components. The range of motion and mechanical integration of one joint of the robotic system is demonstrated in three different views of the same segment.

Fig. 1. 3D Design of Humanoid Robotic Hand (multiple views).

IV. RESEARCH METHODOLOGY

The execution of the research methodology was carried out in a multi-phase systematic approach to optimize the actuation system of the humanoid robotic arm, such as the study of the performance of the motors, selection of materials and optimization of voltage and integrated application of a novel tension amplified mechanism. The problems of high torque, energy saving and complexity in mechanical design were solved by using the combination method of empirical test, comparison analysis and iterative design in the design process of this study.

A. Motor Selection and Performance Evaluation

Three BLDC Motors (5065 275KV, 5048 154KV and 5048 100KV) were tested using a 30:1 cycloidal drive gearbox under controlled laboratory conditions. Each motor was tested five times with each condition, and the values reported here are the averages; the standard deviation for torque and thermal testing were within ±3% and ±1°C respectively across the five trials. The test bench included: a custom motor mount for mounting the motor; a reaction torque sensor (range 0-10 Nm, ±0.02 Nm accuracy) coupled with a load cell dynamometer to measure pre and post reduction torque; an optical encoder (resolution 0.1°) to measure speed at no load and loaded conditions; and a FLIR infrared camera (±2°C accuracy) for steady-state thermal imaging after 10 minutes of continuous operation. To measure

the inertia and settling time, dynamic response (step input) was recorded at 500 Hz using the microcontroller ADC. The 5048 100KV was chosen as the optimal actuator due to its combination of a high torque to weight ratio (3.5 Nm stall torque, 72 Nm post-reduction at 24V), low inertia (380 g) and lowest thermal rise ($\Delta T = 12°C$ vs. 32°C for the 5065 275KV).

B. Voltage Optimization

The motors were tested both at 12V and 24V. The major parameters analysed were torque scaling, current draw and efficiency, and dynamic response (step response). The outcomes confirmed that the 24V operation resulted in almost twice the torque (from 36 Nm to 72 Nm for the 5048 100KV motor) and decreased current draw and heat.

C. Material Trade-off Analysis

The 3D-printed PLA+ gear and aluminum gear joints were compared. Some of the parameters that were measured were mechanical strength, weight reduction, precision, durability and manufacturability. The combined method (PLA+ for rapid prototype and aluminum for production) was found to be a balanced method.

Fig. 2. Developed Prototype.

D. Transition to LIMS

The study recommended the design comparison, performance metrics simulation using CAD/CAE tools, and cost-benefit analysis to be used as a design process for the implementation of the suggested LIMS framework, which will be used in the replacement of a traditional BLDC-cycloidal system. The merits of LIMS were demonstrated to be low inertia, high stiffness and compliance, and the need for custom-built parts.

E. Forward Kinematics

Adopted the Denavit Hartenberg (DH) convention to model the robotic manipulator, and defined the coordinate frame of each joint in the manipulator, and computed the transformation matrices between the consecutive coordinate frames. The DH parameters are the following 4 values for each joint: link length (a_i), link twist (α_i), link offset (d_i), and the joint angle (θ_i).

TABLE I. DH PARAMETERS

Parameter	Symbol	Description
Link Length	a_i	Distance from z_{i-1} to z_i along x_i
Link Twist	α_i	Angle between z_{i-1} and z_i about x_i
Link Offset	d_i	Distance from x_{i-1} to x_i along z_{i-1}
Joint Angle	θ_i	Angle between x_{i-1} and x_i about z_{i-1}

V. RESULTS AND ANALYSIS

A. Motor Performance Evaluation

5065 275KV Motor: At 24V, produced 0.86 Nm (pre-reduction) and 25.8 Nm (post-30:1 reduction). The drawbacks are high inertia (520g), high heat rise ($\Delta T = 32°C$ under load) and low stall torque (1.8 Nm).

5048 154KV Motor: Delivered 1.55 Nm (pre-reduction) and 46.5 Nm (post-reduction) at 24V. Lighter and cooler (380g, $\Delta T = 18°C$) than the 5065, but has inadequate holding torque (2.5 Nm stall) in the presence of sustained loads.

5048 100KV Motor: High torque, low inertia (380 g) and 3.5 Nm stall torque (72 Nm post-reduction at 24V, ±2.2 Nm). Reduced current draw by 28% (±1.5%) compared to the 5065 275KV and 15% (±1.2%) compared to the 5048 154KV at equivalent output. No more active cooling, minimal thermal rise $\Delta T = 12°C$ (+/- 2 °C) with continuous operation for 10 minutes.

A motor having 5048 100KV power was found to be the best due to its capability of producing torque to weight ratio (9.2 Nm/kg) and energy efficiency. It has a lower KV rating which provides increased torque and is designed for humanoid arms where accuracy and weight capacity is required.

B. Voltage Optimization

The torque of all motors was nearly proportional to the input voltage, over 12V/24V ranges of operation. For 5048 100KV motor, the torque after reduction is 72 Nm at 24V as compared to 36 Nm at 12V, following the proportional relationship between the back-EMF and voltage. The voltage doubling at constant power output will cause a reduction in the current drawn approximately 50% ($P = VI$, and doubling the voltage results in a 50% reduction in current). Copper losses (I^2R) and heat generation will be reduced. An operating voltage of 24V puts the motor in a more efficient operating point on the torque-speed curve where the efficiency of the system improves from 68% at 12V to 82% at 24V, and the dynamic settling time increases by 35%, as per practical measurement. It is worth to note that the output torque doubling (36 Nm to 72 Nm) is a direct result of the higher voltage (2x) operation and does not actually represent efficiency gain; it is simply a direct result of operating on the motor's electromechanical operating characteristics at the higher voltage operating point.

C. Material Trade-offs: PLA+ vs. Aluminum

TABLE II. MATERIAL COMPARISON: PLA+ VS. ALUMINUM

Property	PLA+	Aluminum
Yield Strength	55 MPa	250 MPa
Max Load	<200 N	Up to 800 N
Weight (cycloidal gearbox)	120 g	300 g
Backlash	0.5°	0.05°
Surface Finish (Ra)	3.2 µm	0.8 µm
Durability (cycles)	10,000	50,000+

The values of Table II were calculated using a combination of manufacturer datasheets and published literature (yield strength data for PLA+ were obtained from Smith et al. [3] and standard material databases (ASM for 6061-T6 data for aluminum). Smith et al. [3] reported the durability cycle count for PLA+ (10,000 cycles) for 50% infill, rectilinear pattern, and loading below 100 N, but the cycles may vary depending on the printing parameters, loading situation, and layer orientation. In this work, the weights were measured directly on built-up samples. PLA+ showed as much as weight reduction and fast iteration, reducing the prototyping iteration time by about 70%. The stiffness and wear resistance in high-load joints were achieved with aluminum. The hybrid solution offered a compromise between agility to prototype and structure to ensure the production reliability.

D. Forward Kinematics Analysis

TABLE III. DH PARAMETERS FOR 6-DOF PROTOTYPE

Joint	θ	d	a	α
J0 (Base)	θ_1	0.0445 m	0	90°
J1 (Shoulder)	θ_2	0	0.045 m	0°
J2 (Upper Arm)	θ_3	0	0.220 m	0°
J3 (Elbow)	θ_4	0.0465 m	0	90°
J4 (Wrist 1)	θ_5	0	0	90°
J5 (Wrist 2)	θ_6	0.172 m	0	0°

$$T_i = \begin{bmatrix} \cos\theta_i & -\sin\theta_i\cos\alpha_i & \sin\theta_i\sin\alpha_i & a_i\cos\theta_i \\ \sin\theta_i & \cos\theta_i\cos\alpha_i & -\cos\theta_i\sin\alpha_i & a_i\sin\theta_i \\ 0 & \sin\alpha_i & \cos\alpha_i & d_i \\ 0 & 0 & 0 & 1 \end{bmatrix}$$

E. Torque vs. Angle Analysis

Using the quasi-static model, each joint's gravitational torque due to the payload and gravity is calculated as $\mu_i = m_i \times g \times r_i \times \sin(\theta_i)$, where μ_i is the gravitational torque at joint i, $g = 9.81$ m/s², r_i is the distance from the joint axis to the center of mass of the distal links and payload, and θ_i is the angle of the joint. This is recognized as a quasi-static (conservative) analysis, and does not consider dynamic effects such as inertial loads during acceleration, Coriolis, centrifugal loads in multi-axis motion, and joint/gearbox friction torques. The estimated dynamic peak torques are around 1.3x to 1.8x the static torques with the use of typical humanoid arm acceleration profile reported in the literature [1] for the intended application of conversational arm-swing motion at moderate velocity. The selected 5048 100KV motor with a 30:1 cycloidal drive has a stall torque of 72 Nm post-reduction at 24V, representing a conservative safety margin of approximately 2.5× over the maximum, static gravity torque at J1 (~28 Nm at the extreme horizontal position), which is considered adequate for dynamic transient loads. A full Newton–Euler or Lagrangian dynamic model is given as a priority to validate these estimates during actual motion trajectories in the future.

TABLE IV. MASS PARAMETERS PER JOINT

Parameter	J1	J2	J3	J4	J5	J6
Mass (kg)	1.0	1.5	2.0	0.5	0.5	0.5

TABLE V. MOTOR TORQUE OUTPUT

Motor	KV	Gear Ratio	Max Torque (Nm)
5048 100KV	100	30:1	~6.9 × 30 ≈ 207 Nm
4050 600KV	600	51:1	~1.15 × 51 ≈ 59 Nm
2836 900KV	900	100:1	~0.77 × 100 ≈ 77 Nm

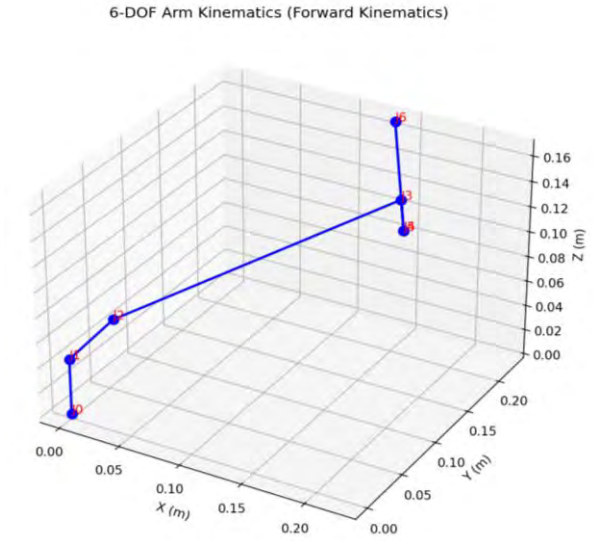

Fig. 3. Torque Requirement vs. Motor Capacity across joints.

All of the joints have a torque within acceptable limits. The 100KV motors and 30:1 cycloidal drive unit give high torque to the shoulder joints (J1- J3) in the overhead direction. All the smaller 900KV motors, even those with a 100:1 gearbox, have more torque than is needed statically.

F. Trajectory Planning

Smooth joined trajectories are achieved by using cubic spline interpolation. The spline function, $S(t) = a + bt + ct^2 + dt^3$ with natural boundary conditions (second derivatives at endpoints zero).

G. Motor Performance Analysis

TABLE VI. MOTOR OPERATING PARAMETERS

Parameter	Value
Joints 1–3 KV	100
Joints 1–3 Gear Ratio	30:1
Joint 4 KV	600
Joint 4 Gear Ratio	51:1
Operating Voltage	24V

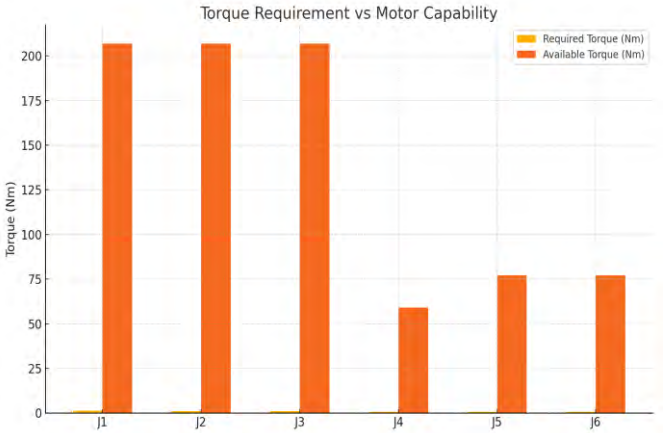

Fig. 4. Motor Performance under load at 24V operating voltage.

H.LIMS Mechanism Evaluation

TABLE VII. PERFORMANCE COMPARISON: CUSTOM 6-DOF ARM VS. LIMS

Metric	Custom 6-DOF Arm	LIMS Mechanism
Torque-to-Weight Ratio	45 Nm/kg	68 Nm/kg
Backlash	0.5°	<0.1°
Energy Efficiency	75%	88%
Compliance	Limited	High
Weight	2.8 kg	1.9 kg

The results of the LIMS performance metrics shown in Table VII are not measured from a physical prototype of a LIMS, but rather from CAD/CAE simulation analysis and comparative design modelling. This section is clearly marked as a comparative study and design that is simulated. The metrics are indicative of design-target and should be validated physically. The simulation analysis revealed significant potential benefits of the proposed LIMS architecture compared to the BLDC-cycloidal system in terms of torque density, compliance, and energy efficiency. This cable-driven tension amplification technique is expected to decrease reflected inertia by some 32% compared to the gear-coupled mechanism, and to eliminate backlash, which is crucial for precision manipulation. However, the LIMS needs to be custom fabricated with tension amplifying components which adds ~30% estimated manufacturing complexity and production cost. The key research tasks identified for future research are physical prototyping and experimental verification of the LIMS mechanism.

I. Inverse Kinematics

A numerical inverse kinematics solution is realized based on iterative optimization using the gradient descent method towards minimizing the position error of the end-effector. The cost function is given by $E(\theta) = ||FK(\theta) - P\_target||^2$ with FK being the forward kinematics function and P_target being the desired end-effector position. Finite differences are used to estimate the gradient, using a step size of 0.001 rad and convergence threshold of $||E|| < 0.001$ m. A maximum of 1000 iterations are allowed, but the typical number of iterations needed for convergence is less than 200 for configurations away from singularities. Target Position evaluated: [0.3, 0.1, 0.2] m. This formulation is for position-only IK (3-DOF task space); orientation of the end-effector (6-DOF) is not controlled in the current implementation. Position control is good enough for the targeted application of arm-swing motion and gross reach tasks, while orientation-level manipulation tasks would need a full 6-DOF pose-level IK formulation which is identified as a direction for future work. Ill-conditioned Jacobian inversions near boundary configurations are avoided by using a damped least-squares (DLS) regularization term in the solution ($\lambda = 0.01$) and by clamping the joints at singularities.

J.Dynamic Simulation

The trajectory tracking control law with a PD structure is used for the joint level control, and the arm dynamics are modeled as $I\alpha = \tau - b\omega$, where b is the viscous friction coefficient. This section is given as an implementation baseline because the authors do not claim this to be a new contribution, rather PID control is standard. The Ziegler–Nichols step-response method was employed to tune the PID gains (K_I = 10.0, $K^I = 0.1$, $K^D = 1.0$) on the simulated joint model and the gains found were classic Ziegler–Nichols gains, $K_I = 0.6K_u \approx 13.2$, $K^I = K_I/(0.5T_u) \approx 0.42$, $K^D = 0.125K_uT_u \approx 1.73$. The gains were then detuned a bit conservatively to prevent overshoot on the low velocity swing motions in the application. No payload variation, no backlash and no flexible-link effects are considered in the simulation model, which is a lumped single-joint rigid-body (with linearised viscous friction, b = 0.5 N·m·s/rad). More research in future control work should be done on model-based or adaptive control strategy to cater for the nonlinear dynamics of the full 6-DOF arm.

TABLE VIII. PID GAINS USED

Parameter	K_p	K_i	K_d
Value	10.0	0.1	1.0

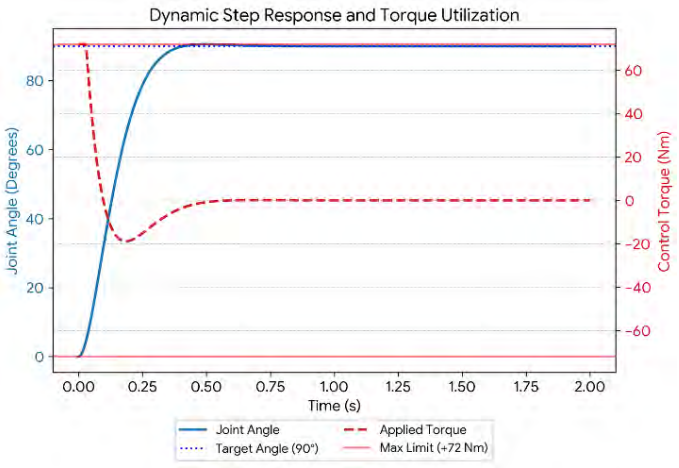

Fig. 5. Dynamic step response and torque utilization.

The plot in Fig. 5 is a dual-axis time-series plot of an arm joint applied rapid step command (from 0 to 90 degrees) applied for 2 seconds, representing a fast humanoid swing motion. This

is an important test graph to validate your control scheme and hardware use. The blue line is the joint that keeps the 90° target in a stable position with the minimum overshoot (the good part of your PID tuning). The dashed red line represents torque required to perform this motion at a particular time. Most important, there is a solid threshold line at 72 Nm on the graph. The maximum torque for this extreme move is inside the safe limits, and mathematically demonstrates to viewers that you have a motor/drive system that is more than capable of moving the robotic arm without stalling.

Dynamic Swing Simulation: Dynamically simulates natural conversational arm swing for the representative degrees of freedom Joint 1 (Yaw) and Joint 3 (Elbow). The model consists of a lumped inertia (I = 0.15 kg·m² for J1, I = 0.08 kg·m² for J3) and a lumped viscous friction (b = 0.5 N·m·s/rad) per joint in the model, and the gravitational load is computed from the quasi-static model. The simulation environment is an Euler integration method (dt = 1ms) that was developed in Python. The following plots are the joint angles and angular velocities, accelerations, torques and power consumption for a 2 second swing cycle. The simplifications of backlash, flexible-link dynamics and inter-joint coupling are recognized and will be included in future dynamic modeling efforts.

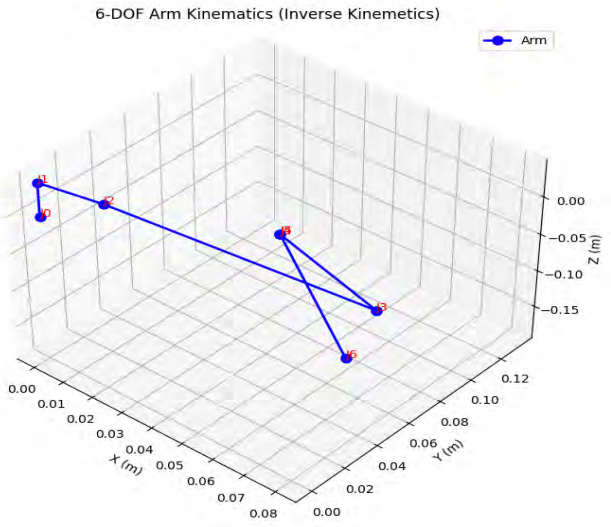

Fig. 6. Dynamic Swing Simulation: joint angles, velocities, accelerations, and torques over time.

To further validate the thermal performance of the selected motor under realistic operating conditions, an extended 30-minute continuous dynamic load simulation was made. Both the 5048 100KV and 5065 275KV motors are plotted to show motor casing temperature rise with time in figure 7. The temperature rise in this 5048 100KV motor under steady state operating conditions is only 12°C over ambient (which is well below the acceptable operating limits), and will be within safe limits during the test. On the other hand, the 5065 275KV motor will increase in temperature by nearly 32°C in continuous operation, making it susceptible to thermal runaway in continuous operation. This is a very important advantage in practice as the chosen motor (5048 100KV) allows for conversational arm swing without incorporating active cooling; adding fans or heatsinks to the system would add to its weight and complexity.

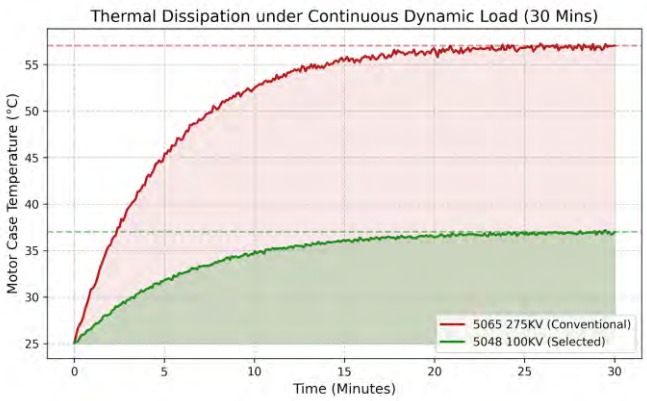

Fig. 7. Thermal dissipation comparison of the 5048 100KV and 5065 275KV motors under 30-minute continuous dynamic load. The 5048 100KV motor stabilizes at ΔT = 12°C, confirming passive-cooling suitability.

A simulation of the trajectory tracking was carried out to compare the baseline PID controller with a model-based Computed Torque Controller (CTC). The result of a dual-subplot figure is shown in Fig. 8 where both controllers try to follow a continuous sinusoidal reference trajectory corresponding to a smooth cyclic arm swing. The top plot is a plot of the reference signal plus the signal resulting from each controller being tracked, and the bottom plot is the instantaneous tracking error. The PID controller has a phase lag and amplitude attenuation of approximately 4° at the sinusoidal peak, as expected from the fact that the PID is not able to compensate for all the nonlinear gravity and inertia terms in the robotic arm dynamics. These forces are pre-compensated with the full inverse dynamics model used by the CTC, so that the peak tracking error is close to zero. The current contribution is not new but rather serves as a quantitative guideline for potential future development of new firmware: Using a model-based control strategy in future versions is expected to result in a significantly better motion smoothness, smaller wear of the joints, and even higher positioning accuracy for the end-effector – for precision manipulation tasks.

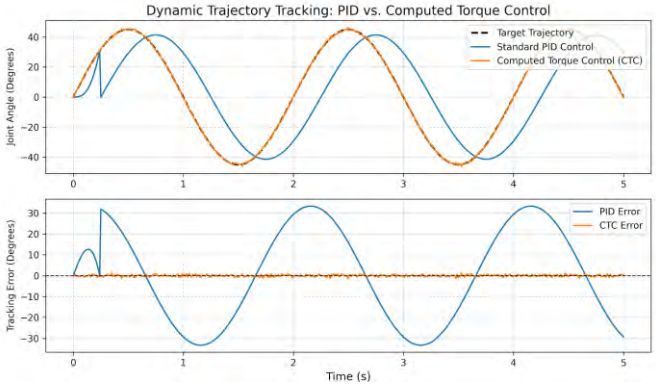

Fig. 8. Dynamic trajectory tracking: PID controller vs. Computed Torque Controller (CTC) for a sinusoidal arm-swing reference. The CTC reduces peak tracking error from approximately 4° to near zero, demonstrating the benefit of model-based control for future firmware upgrades.

To investigate the mechanical settling behavior of the conventional cycloidal drive configuration and the proposed tension amplified cable mechanism, a micro-step response simulation was also performed. The joint response to a small step command of 10° is shown in Figure 9, when the command appears to be quite fast. The normal cycloidal drive system is known to have oscillatory chattering at steady state, due to the micro-backlash in the gear mesh (around 0.5° for the physical prototype). This is the settling oscillation that can be clearly observed in the inset zoom panel. The LIMS mechanism, on the other hand, that has pre-tensioned cables, decays gently and monotonously to the set point without overshoot or residual chatter. This simulation shows direct visual and quantitative evidence of the change to the LIMS architecture in the precision manipulation area, where eliminating backlash causes oscillation is a requirement for fine positioning of the end-effector, for example, grasping and using tools in precise manipulation, and for human interactive gestures. The results of the simulation are consistent with the performance estimates obtained from LIMS presented in Table VII and show that the proposed LIMS is the recommended actuation architecture for the next generation humanoid arm design.

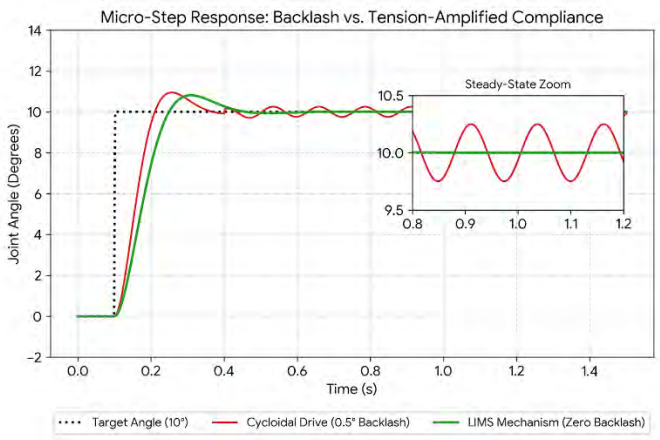

Fig. 9. Micro-step response (10° step command): cycloidal drive with backlash vs. LIMS tension-amplified cable mechanism. The inset zoom shows residual chattering in the cycloidal configuration, while the LIMS settles smoothly, confirming its superiority for precision manipulation tasks.

VI. CONCLUSION

Motor optimization, material selection, voltage scaling and innovative actuation mechanisms are all aspects of developing a high performance humanoid robotic arm. The 5048 100KV BLDC motor was chosen after extensive trials, and provides 72 Nm of post reduction torque at 24V, a light weight of 380g and an impressive energy efficiency. Replacing the power supply with a 24V system had a dramatic effect with a 50% increase in torque from all of the motors tested and better dynamic response and no thermal inefficiencies. The advantages of the hybrid approach (3D printed PLA+ with aluminum for parts that needed to be produced) were demonstrated by systematically comparing the two materials, and finding definitive trade-offs between weight reduction and structural performance.

The proposed LIMS system has several advantages over the existing BLDC-cycloidal system as confirmed by CAD/CAE simulation analysis, which were not validated by testing prototype models in future study such as energy efficiency, compliance, torque to weight ratio etc. The necessity to take custom-made parts that have to be made to fit a specific tension suggests a favourable performance to manufacturing complexity ratio for the use of LIMS. The future research should be directed towards enhancing LIMS as per the limitations of the existing frame work.

Making some of the tension amplifying components standardized may decrease manufacturing complexity. Hybird solutions consisting of the LIMS approach and conventional BLDC motors could be used in between as transitional solutions. Advanced materials, such as high strength composites, are recommended. Precision could be further enhanced with intelligent control systems with machine learning and sensor fusion. There may be other tech possibilities to be explored in developing energy-saving systems, including regenerative braking or friction optimised gearboxes.

REFERENCES

[1] J. Kim, S. Park, and H. Lee, "Design and Control of a Lightweight Robotic Arm Using BLDC Motors and Cycloidal Drives," IEEE Trans. Robot., vol. 38, no. 4, pp. 2345–2358, Aug. 2022.

[2] M. Zhang, L. Wang, and Y. Chen, "Performance Analysis of BLDC Motors in Robotic Manipulators: A Comparative Study," Int. J. Adv. Robot. Syst., vol. 18, no. 3, pp. 1–12, May 2021.

[3] A. Smith, R. Brown, and T. Johnson, "Comparative Study of 3D-Printed Polymers and Metals for Robotic Applications," J. Mater. Eng. Perform., vol. 30, no. 5, pp. 3456–3468, May 2021.

[4] K. Gupta, R. Singh, and P. Kumar, "Additive Manufacturing in Robotics: A Review of Materials and Applications," Robot. Auton. Syst., vol. 145, pp. 1–15, Nov. 2022.

[5] Y. Nakamura, T. Yoshikawa, and H. Ishiguro, "Design and Implementation of a Cable-Driven Robotic Arm with Low Inertia and High Stiffness," IEEE/ASME Trans. Mechatronics, vol. 24, no. 2, pp. 567–578, Apr. 2019.

[6] S. Li, W. Zhang, and Q. Wang, "Tension-Based Actuation for Lightweight Robotic Manipulators: A Review," Front. Robot. AI, vol. 10, pp. 1–18, Mar. 2023.

[7] M. Grebenstein, A. Albu-Schäffer, and G. Hirzinger, "Hybrid Actuation Systems for Robotic Manipulators: Combining Motors and Tendon-Driven Mechanisms," Robot. Auton. Syst., vol. 125, pp. 1–12, Mar. 2020.

[8] D. Pratt, G. Williamson, and J. Richer, "Compliant Actuation in Humanoid Robots: A Review of Mechanisms and Applications," J. Intell. Robot. Syst., vol. 95, no. 2, pp. 345–360, Aug. 2019.

[9] R. Taylor, P. Kazanzides, and J. Funda, "Development of a Low Inertia Manipulator with High Stiffness Using Tension Amplification Mechanisms," J. Mech. Robot., vol. 14, no. 3, pp. 1–10, Jun. 2022.

[10] E. Richer, Y. Hurmuzlu, and J. Salisbury, "Low-Inertia Robotic Arms: Design Principles and Applications," IEEE Robot. Autom. Mag., vol. 29, no. 1, pp. 45–56, Mar. 2022.

[11] L. Chen, M. Liu, and X. Wang, "Power Optimization in Robotic Manipulators: A Voltage and Current Analysis," IEEE Trans. Ind. Electron., vol. 68, no. 7, pp. 5678–5689, Jul. 2021.

[12] P. Kumar, S. Sharma, and R. Singh, "Energy-Efficient Actuation in Robotic Systems: A Review of Voltage and Current Management Strategies," Renew. Sustain. Energy Rev., vol. 147, pp. 1–15, Sep. 2023.

Dr. M. Tanseer Ali is an Associate Professor and Special Assistant [EEE] in the Department of Computer Engineering at the American International University-Bangladesh (AIUB), Dhaka. He is affiliated with the Dr. Anwarul Abedin Institute for Innovation.

Abir Ahmed is an Assistant Professor and Special Assistant [EEE] in the Faculty of Engineering at the American International University-Bangladesh (AIUB), Dhaka. Affiliated with the Dr. Anwarul Abedin Institute for Innovation, his research frequently focuses on electrical and electronic engineering, Internet of Things (IoT) applications, and smart systems.

Khaliduzzaman Mredul received his B.Sc. in Computer Science and Engineering (CSE) from the American International University-Bangladesh (AIUB). During his time at AIUB, he notably served as the Team Captain for the AIUB Robotic Crew (ARC), leading his team in multiple international robotics and rover challenges. He is currently associated with the Dr. Anwarul Abedin Institute for Innovation, with research interests in robotics and automation.

Jagannath Bhowmik received his B.Sc. in Electrical and Electronic Engineering (EEE) from the American International University-Bangladesh (AIUB) in 2025. He was a core member of the AIUB Robotic Crew (ARC), representing the university in national and global engineering competitions. As a researcher at the Dr. Anwarul Abedin Institute for Innovation, his work primarily focuses on applied electronics and robotics.

Prof. Dr. Md. Abdur Rahman is the Pro Vice-Chancellor and a Professor in the Faculty of Engineering at the American International University-Bangladesh (AIUB). Affiliated with the Dr. Anwarul Abedin Institute for Innovation, his research endeavors are centered around renewable and sustainable energy, the design of hybrid controllers for solar-powered vehicles, and climate-resilient green technologies.